

## GROWTH AND IR SPECTRA OF YAG AND ND: YAG SINGLE CRYSTALS

### RAST I IR SPEKTRI MONOKRISTALA YAG I ND:YAG

ALEKSANDAR GOLUBOVIĆ,\* SLOBODANKA NIKOLIĆ,\*  
RADOŠ GAJIĆ,\* ZORANA DOHČEVIĆ-MITROVIĆ\* ANDREJA VALČIĆ\*\*

\**Institute of Physics, Zemun-Belgrade, Serbia and Montenegro*, and  
\*\**Faculty of Technology and Metallurgy, Belgrade, Serbia and Montenegro*

Primljeno: 11. 10. 2004.

#### ABSTRACT

$Y_3Al_5O_{12}$  (YAG) and doped with 0.8 % wt. Nd (Nd:YAG) single crystals were grown by the Czochralski technique under an argon atmosphere. The conditions for growing Nd:YAG and YAG single crystals were calculated by using a combination of Reynolds and Grashof numbers. The critical crystal diameter and the critical rate of rotation were calculated from the hydrodynamics of the melt. Optical spectra of Nd:YAG and YAG single crystals were recorded in the range 50-4000  $cm^{-1}$  at various temperatures. TO and LO modes were calculated using Kramers-Kronig analysis. The obtained results were discussed and compared with published data.

**Key words:** Czochralski technique, Nd:YAG, YAG, growth, single crystal, optical spectra

#### IZVOD

Monokristali  $Y_3Al_5O_{12}$  (YAG) i dopirani sa 0,8 tež. % Nd (Nd:YAG) rasli su u argonu pomoću tehnike po Čohralskom. Kombinacijom Rejnoldsovog i Grashofovog broja su izračunati uslovi za rast monokristala Nd:YAG i YAG. Vrednosti kritičnog prečnika kristala i kritične brzine rotacije su izračunate korišćenjem jednačina dinamike fluida. Optički spektri monokristala Nd:YAG i YAG su snimljeni na različitim temperaturama u opsegu od 50-4000  $cm^{-1}$ . TO i LO modovi su izračunati Kramers-Kronig analizom. Dobijeni rezultati su diskutovani i poređeni sa literaturnim podacima.

**Ključne reči:** tehnika po Čohralskom, Nd:YAG, YAG, rast, monokristal, optički spektri.

#### INTRODUCTION

Oxide crystals are solid-state materials which have had very attractive properties for the generation, transmission, detection, and conversion of optical signals over a broad range of wavelength and power level [1, 2]. There has been a continuing interest in the development of  $Y_3Al_5O_{12}$  (YAG) crystal growth technology because Nd-doped YAG is one of the most important laser hosts for

the generation of 1.06  $\mu$  infra-red radiation [3]. The garnet host is a cubic crystal with space group Ia3d. It has high mechanical strength, good chemical stability, and the ability to be synthesized in large sizes with high optical quality [4]. Nd:YAG crystals are usually grown by the conventional Czochralski (CZ) technique [5-8]. Besides that, for miniature laser sources Nd:YAG can grow by the micropulling-down ( $\mu$ -PD) technique [9, 10] and by the crucibleless laser heating pedestal method [11-13].

The shape of melt/crystal interface is strongly affected by internal radiant heat transfer through the crystal and this mechanism promotes deeply deflected interfaces toward the melt.<sup>14</sup> The deep interfaces in these systems can lead to detrimental features in the grown crystal, notably the production of highly strained regions near the core of the crystal, which correspond to facet formation along the melt/crystal interface during growth [15, 16]. The appearance of a core is typical for Bi<sub>12</sub>SiO<sub>20</sub>, Bi<sub>12</sub>GeO<sub>20</sub> and Nd:YAG crystals. Applying both theoretical and experimental investigations, we successfully obtained all of these single crystals without a core [8, 17, 18]. It was predicted in the literature<sup>4</sup> that the width and position of the Nd:YAG spectral lines vary with temperature. The aim of our work was, by applying both theoretical and experimental treatment, to produce and characterize YAG single crystals with and without dopant Nd<sup>3+</sup> without a core, and obtain optical properties using IR spectra.

## EXPERIMENTAL

Yttrium aluminium garnet single crystals with and without dopant neodymium (Nd:YAG and YAG) were grown by the Czochralski technique using a MSR 2 crystal puller, as described previously [8]. The atmosphere used was argon. The iridium crucible ( $\varnothing$  4 cm, 4 cm depth), was placed into an alumina vessel surrounded by ZrO<sub>2</sub> wool isolation. Double walls were used to protect the high radiation. To decrease the radial temperature gradient in the melt, alumina was mounted around all the system. The pull rates were generally in the range 0.8-3 mm/h, and the best results were obtained with a pull rate of 1 mm/h. The critical crystal rotation was calculated to be 20 rpm. The crystal diameter was set and automatically kept constant by an additional weighing assembly that continuously monitored the crucible weight. The critical diameter of crystal was calculated to be 15 mm. The crucible was not rotated during the growth. After the growth run, the crystal boule was cooled at a rate of about 50 K/h down to room temperature.

All obtained crystal plates were checked in polarised light to reveal strains.

The chemical compositions of the products were determined by the XRD powder technique. All samples were examined under the same conditions, using a Philips PW 1729 X-ray generator, a Philips 1710 diffractometer and the original APD software. The radiation source was an X-ray LFL tube with copper radiation and a graphite monochromator. The radiation was  $\lambda$ CuK $\alpha_1$  = 0.15405 nm. The anode tube load was 40 kV and 30 mA. Slits of 1.0 and 0.1 mm were fixed. Samples were pressed into standard aluminium frames and

measured in the  $2\theta$  ranges from  $10^\circ$  to  $100^\circ$ . Each  $1/50^\circ$  ( $0.02^\circ$ ) was measured for 0.5 s. For production identification, the MPDS program and JCPDS (ASTM) card files were used.

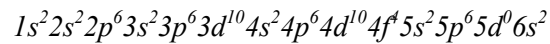
The infrared spectra were recorded on a Bomem DA8 Fourier-transform spectrometer. A new hyper splitter was used for the far infrared region (from  $20$ - $700\text{ cm}^{-1}$ ) and a standard KBr ( $400$ - $5000\text{ cm}^{-1}$ ) beamsplitter for the infrared region. All the spectra were obtained for a near normal incidence configuration at different temperatures ( $T = 80\text{ K}$ , and  $298\text{ K}$ ). A Globar (SiC) source was used in both regions of the infrared spectra. All measurements were performed using a Janis STDA 100 cryostat, which enabled the precise exchange of the sample and the mirror in the same position of the cold finger. At the lower temperature, a polyethylene (far IR) and ZnSe (mid IR) window were used. Liquid nitrogen ( $\text{LN}_2$ ) was used as the coolant. A Lake Shore 330 temperature controller provided a temperature error within  $0.1\text{ }^\circ\text{C}$ .

## RESULTS AND DISCUSSION

Refractory oxide crystals exhibit some degree of transparency to infrared radiation, and this effect greatly influences heat transfer during Czochralski growth. The shape of the melt/crystal interface is strongly affected by internal radiant heat transfer through the crystal, and this mechanism promotes deeply deflected interface toward the melt [14]. The deep interfaces in these system can lead to deleterious features in the growth crystal, notably the production of highly strained regions near the core of the crystal which correspond to facet formation along the melt/crystal interface during growth [19]. During the growth of oxide crystals, there are two main opposing forces within the crucible, the buoyancy driven convection flow due to temperature gradient in the bulk melt and the centrifugal force driven by the rotation of the crystal [20]. It was presumed, as Carruthers [21] did, that there was not change in kinematic viscosity at the interface melt/crystal during the process of the growth and there was equilibrium  $\text{Gr}=\text{Re}^2$ . There is, in this time, a flat interface melt/crystal with critical rotation rate  $\omega_c$  and critical diameter  $d_c$ . We decided to use the relations derived by Carruthers in calculations for our experimental system. These relations are in a good agreement with the experimental data of many authors [22-24] for crystals with a high Prandtl number and we assumed that it could also be useful in our case. In this way, by applying the hydrodynamic forms, crystal necking values for the critical diameter  $D_c = 1.5\text{ cm}$  and the critical rotation rate  $\omega_c = 28\text{ rpm}$  were found. At the bottom of the crystal,  $\omega_c = 13\text{ rpm}$  was calculated to be. The rotation rate of the crystal was programmed to decrease linearly with the melt height from about  $28\text{ rpm}$  at the start to about  $13\text{ rpm}$  at the end of the pulling. The pulling rate was experimentally found to be  $0.8$ - $1.0\text{ mm/h}$ . Flat-interface growth of YAG is difficult to achieve, especially for neodymium-doped material. However, it was reported [14, 25] that flat-interface Nd:YAG single crystals growth can be achieved by applying a low thermal gradient. Xu et al. [25] employed a massive baffle over the melt to

promote extreme thermal gradients, while Xiao et al.<sup>14</sup> use a two-zone furnace. For this purpose, we used an alumina tube in our crystal growth experiments.

The electronic configuration for the 60 electrons of a neodymium atom is [4]:



where the first nine sets of orbital make up the filled core, while the optically active electrons are in the partially filled 4f orbital. The latter are shielded by the electrons in the outermost 5s through 6s orbital. The trivalent neodymium ion has given up three electrons, two from the outer 6s orbital and one from the 4f orbital, leaving a configuration of (Xe)4f<sup>3</sup>5s<sup>2</sup>5p<sup>6</sup>. The three 4f electrons are the ones that play the dominant role in determining the optical properties of the ion.

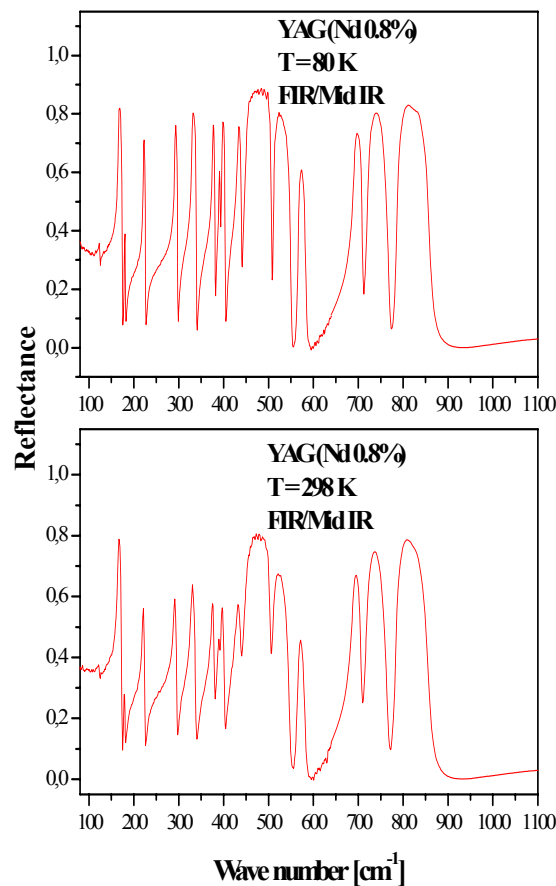


Figure 1: Reflectance spectra of Nd:YAG single crystal in the range 80-1100 cm<sup>-1</sup> at T=80 K and T=298 K

The yttrium ion is surrounded by eight oxygen ions in the shape of a distorted cube [4]. The Nb<sup>3+</sup> ions substitute for Y<sup>3+</sup> in YAG without the need for

charge compensation. The larger size of the  $Nb^{3+}$  ion results in polyhedra with sides that are greater than those in  $Al^{3+}$  polyhedra. That distorts the lattice and thus limits the maximum doping concentration to several atomic weight percent. Concentration of  $Nd^{3+}$  in our samples is, as a common for laser materials, 0.8 wt. %. The lattice strains that are introduced by doping affect the properties of the optical spectra.

Optical spectra of Nd:YAG and YAG single crystals were recorded in mid IR and far IR region at room temperature (298 K) and at temperature of liquid nitrogen (80 K). The reflectance spectra of both single crystals are similar in the range  $50-1900\text{ cm}^{-1}$ , position of peaks are almost in the same place. Reflectance spectra of Nd:YAG single crystal at both temperatures is shown in Figure 1.

Electron-phonon interactions have a significant affect on the optical spectra of  $Nd^{3+}$  ions in YAG. Factor group analysis of YAG crystal predicts 98 vibrational modes for  $k=0$  phonons. Infrared spectra show vibrational transitions ranging between  $120$  and  $920\text{ cm}^{-1}$ . This gives the energy range of phonons available for thermal line broadening, line shifting, and radiation less decay processes.<sup>4</sup> After the Kramers-Kronig analysis of the spectra YAG and Nd:YAG single crystals at 80 K and 295 K, the positions of TO and LO modes were obtained. There are not practically shifting in the case of YAG crystal, while Nd:YAG crystal do. Positions of TO and LO are presented in Tables I and II.

*Table I: The transverse (TO) frequencies of the optical phonons for Nd:YAG single crystals in the range  $100-950\text{ cm}^{-1}$  at  $T=80\text{ K}$  and  $T=298\text{ K}$ .*

Number of phonon mode	Position of phonon mode at $T=80\text{ K}$ , [ $\text{cm}^{-1}$ ]	Position of phonon mode at $T=298\text{ K}$ , [ $\text{cm}^{-1}$ ]
1	121	119
2	165	164
3	178	176.5
4	220.5	218.5
5	291	288.5
6	329	327
7	375	373
8	389	387
9	396	394
10	431	429.5
11	450	446
12	511	510
13	567	564.5
14	689	684
15	720	716
16	785	781

Clear differences appear in the infrared spectra where there are some peaks in Nd:YAG single crystal, while there are absent in YAG single crystal. This effect is shown in Figure 2, while Figure 3 shows this range of Nd:YAG spectra at both temperatures.

Table II: The longitudinal (LO) frequencies of the optical phonons for Nd:YAG single crystals in the range 100-950  $\text{cm}^{-1}$  at  $T=80\text{ K}$  and  $T=298\text{ K}$

Number of phonon mode	Position of phonon mode at $T=80\text{ K}$ , [ $\text{cm}^{-1}$ ]	Position of phonon mode at $T=298\text{ K}$ , [ $\text{cm}^{-1}$ ]
1	124	123
2	174	172
3	181	180
4	225.5	223.5
5	297.5	295
6	338.5	336.5
7	380.5	378.5
8	392.5	390.5
9	403	401
10	439	437
11	506	502
12	549.5	545.5
13	583	581
14	710	707.5
15	768.5	765
16	856	851

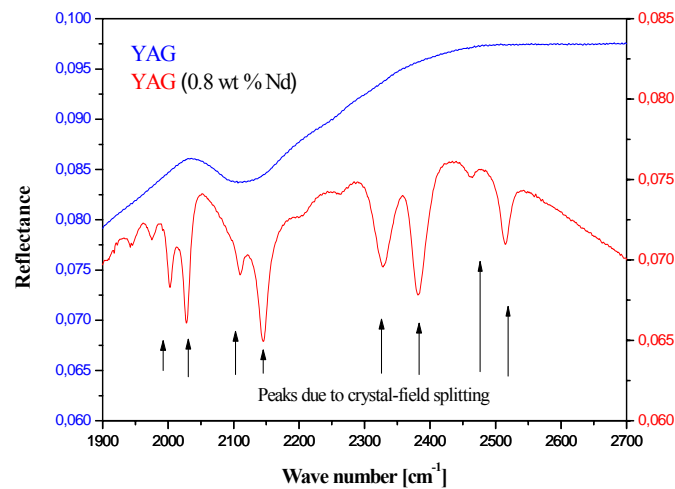


Figure 2: Reflectance spectra of Nd:YAG and YAG single crystal in the range 1900-2700  $\text{cm}^{-1}$  at  $T=298\text{ K}$

Positions of six peaks can be explained by the spin-orbit interaction where energy levels of the lowest terms of the  $\text{Nd}^{3+}$  ions, and the crystal-field splitting of the lowest levels in a YAG host crystal.<sup>4</sup>  $^4I_{11/2}$  split in six levels from 2002 to 2511  $\text{cm}^{-1}$ , but peaks at 2334 and 2389  $\text{cm}^{-1}$  does not belong to this splitting. To the best of our knowledge, the positions of these peaks in Nd:YAG spectra have not been published in the literature, and we suppose that they belong to energy level of the higher terms of  $\text{Nd}^{3+}$  ions. Peaks at 3922 and 3930  $\text{cm}^{-1}$  belong to  $^4I_{13/2}$  splitting (two of seven, where the other appears after 4000  $\text{cm}^{-1}$ ).

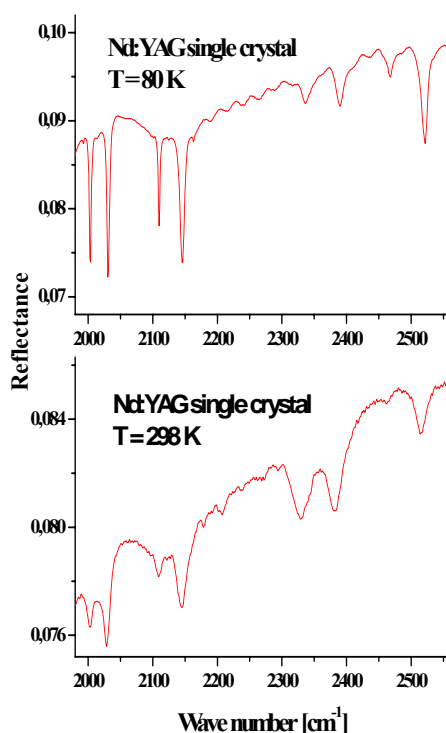


Figure 3: Reflectance spectra of Nd:YAG single crystal in the range 1980-2560  $\text{cm}^{-1}$  at  $T=80\text{ K}$  and  $T=298\text{ K}$ .

### CONCLUSION

The conditions for growing Nd:YAG single crystals were calculated by using a combination of Reynolds and Grashof numbers. From the hydrodynamics of the melt, the critical crystal diameter  $D_c = 1.5\text{ cm}$  and the critical rate of rotation changed from  $\omega_c = 38\text{ rpm}$  after necking to  $\omega_c = 13\text{ rpm}$  at the end of the crystal. The value of the rate of crystal growth was experimentally found to be 0.8-1.0 mm/h.

The values of 16 active infrared modes are revealed in Nd:YAG reflectance spectra both at 80 K and at 298 K by the Kramers-Kronig analysis.

It was found peaks due to crystal-field splitting in Nd:YAG spectra at wave numbers range from 2002 to 2511  $\text{cm}^{-1}$ . Six peaks belong to  $^4I_{11/2}$  the crystal-field splitting of the lowest levels in a YAG host crystal. Additional two at 2334 and 2389  $\text{cm}^{-1}$  probably belong to energy level of the higher terms of  $\text{Nd}^{3+}$  ions.

### ACKNOWLEDGEMENT

This work is supported by Serbian Ministry of Science, Technology and Development under Projects 1469 and 1481.

## REFERENCES

- [1] T. Fukuda, K. Shimamura, V. V. Kochurikhin, V. I. Chani, B. M. Epelbaum, S. L. Buldochi, H. Takeda, A. Yoshikawa, *J. Mat. Science: Mat. Electron.* **10** (1999) 571
- [2] D. Jun, D. Peizhen, X. Jun, *J. Cryst. Growth* **203** (1999) 163
- [3] V. I. Chani, A. Yoshikawa, Y. Kuwano, K. Hasegawa, T. Fukuda, *J. Cryst. Growth* **204** (1999) 155
- [4] R. C. Powell, *Physics of Solid-State Laser Materials*, ed. G. W. F. Drake, Springer Verlag, New York, Berlin, Heidelberg, 1998
- [5] C. Belouet, *J. Cryst. Growth* **15** (1972) 188
- [6] V. J. Fratello, C. D. Brandle, *J. Cryst. Growth*, **128**, (1993) 1006
- [7] Z. Gałazka, H. Wilke, *J. Cryst. Growth* **216** (2000) 389
- [8] A. Golubović, S. Nikolić, R. Gajić, S. Đurić, A. Valčić, *J. Serb. Chem. Soc.* **67** (2002) 291
- [9] Y. M. Yu, V. I. Chani, K. Shimamura, T. Fukuda, *J. Crystal Growth* **171** (1997) 463
- [10] Y. M. Yu, V. I. Chani, K. Shimamura, K. T. Inaba, T. Fukuda, *J. Crystal Growth* **177** (1997) 74
- [11] R. S. Feigelson, *J. Crystal Growth* **79** (1986) 669
- [12] R. S. Feigelson, *Mater. Sci. Eng. B* **1** (1988) 67
- [13] R. S. Feigelson, "Tunable Solid State Lasers I", Edts. P. Hammerling, A. B. Budgor, A. Pinto, Springer Verlag, Berlin-Heidelberg-New York-Tokyo, 1985, pp. 129-142
- [14] Q. Xiao, J. J. Derby, *J. Crystal Growth* **139** (1994) 147
- [15] K. Kitamura, S. Kimura, Y. Miyazawa, Y. Mori, O. Kamada, *J. Crystal Growth* **62** (1983) 351
- [16] S. E. Stokowski, M. H. Randles, R. C. Morris, *IEEE J. Quantum Electron* QE-**24** (1988) 934
- [17] A. Golubović, S. Nikolić, R. Gajić, S. Đurić, A. Valčić, *J. Serb. Chem. Soc.* **64** (1999) 553
- [18] A. Golubović, S. Nikolić, R. Gajić, S. Đurić, A. Valčić, *Hem. ind.* **53** (1999) 227 (in Serbian)
- [19] V. Vaithianathan, S. Kumaragurubaran, N. Senguttuvan, P. Santhana-  
raghavan, I. Ishii, P. K. Sinha, P. Ramasamy, *J. Crystal Growth* **235**  
(2002) 212
- [20] S. Kumaragurubaran, S. M. Babu, K. Kitamura, S. Takegawa, C. Subra-  
manian, *J. Crystal Growth* **229** (2001) 223
- [21] J. R. Carruthers, *J. Crystal Growth* **36** (1976) 212
- [22] D. C. Brown, *IEEE J. Quantum Electron.* **34** (1998) 2393
- [23] V. J. Fratello, C. D. Brandle, *J. Crystal Growth* **128** (1993) 1006
- [24] M. Berkowski, K. Iliev, V. Nikolov, P. Peshev, W. Piekarczyk, *J. Crystal  
Growth* **83** (1987) 507
- [25] T. Xu, Z. Wu, W. Peng, Q. Zhen, Z. Xiao, J. Zhou, S. Zhang, S. Xie, C.  
Huang, Q. Zhou, *Proc. 10<sup>th</sup> Int. Conf. On Crystal Growth*, San Diego,  
California, USA, 1992, p. 10